

PV Based Multifunctional DVR Implementation for Emergency Control in Distribution Systems by using Z Source Inverter

¹VINAY KUMAR KUCHANA, ²GUNDU POORNA

^{1,2}Assistant Professor

Department of Electrical & Electronics Engineering,
Bhoj Reddy Engg College for Women, Telangana, India.

Abstract This paper proposes a photovoltaic (PV) system, which exhibits a set of benefits when draw parallels to conventional stand-alone PV system. In the present system, the generated energy by the PV arrays is managed by multi-string step-up converters. Voltage swell and sag is big brain-teasers in power system. Sensitive load has a serious effect on itself due to voltage swell and sag. Dynamic Voltage Restorer (DVR) is a power conventional appliance used in power distribution network. Various equivalent circuit models of a PV cell have been proposed. For obtaining high power, numerous PV cells are connected in series and parallel on a panel, which is a PV module. The dynamic voltage restorer with its excellent dynamic capabilities, when installed between the supply and critical load feeders, Power distribution system should ideally provide their customers an uninterrupted flow of energy with smooth sinusoidal voltage at the contracted magnitude and frequency.

A Z-source inverter is a type of power inverter, a circuit that converts direct current to alternating current. The impedance network composed of split inductors and two capacitors. The supply can be DC voltage source or DC current source or AC source. Z-source inverter can be of current source type or voltage source type. Z-Source inverter operation is controlled by multiple pulse width modulation. The output of the Z-Source inverter is controlled by using pulse width modulation, generated by comparing a triangular wave signal with an adjustable DC reference and hence the duty cycle of the switching pulse could be varied to synthesize the required conversion. DVR can be considered to be cost effective when compared with other compensation devices. But the use of DC link capacitor in the conventional DVR will increase the size, weight and the cost of the entire system which inhibits widespread use of DVR. The dynamic voltage restorer is one of the modern devices used in distribution systems to protect consumers against sudden changes in voltage amplitude. The simulation results are obtained using MATLAB/SIMULINK software

Index Terms—Dynamic voltage restorer (DVR), emergency control, voltage sag, voltage swell, PV system, Z-source inverter.

I. INTRODUCTION

VOLTAGE sag and voltage swell are two of the most important power-quality (PQ) problems that encompass almost 80% of the distribution system PQ problems [1]. According to the IEEE 1959–1995 standard, voltage sag is the decrease of 0.1 to 0.9 p.u. in the rms voltage level at system frequency and with the duration of half a cycle to 1 min [2]. Short circuits, starting large motors, sudden changes of load, and energization of transformers are the main causes of voltage sags [3].

According to the definition and nature of voltage sag, it can be found that this is a transient phenomenon whose causes are classified as low- or medium-frequency transient events [2]. In recent years, considering the use of sensitive devices in modern industries, different methods of compensation of voltage sags have been used. One of these methods is using the DVR to improve the PQ and compensate the load voltage [6]–[13].

Previous works have been done on different aspects of DVR performance, and different control strategies have been found. These methods mostly depend on the purpose of using DVR. In some methods, the main purpose is to detect and compensate for the voltage sag with minimum DVR active power injection [4], [5]. Also, the in-phase compensation method can be used for sag and swell mitigation [6]. The multiline DVR can be used for eliminating the battery in the DVR structure and controlling more than one line [7], [14]. Moreover, research has been made on using the DVR in medium level voltage [8]. Harmonic mitigation [9] and control of DVR under frequency variations [10] are also in the area of research. The closed-loop control with load voltage and current feedback is introduced as a simple method to control the DVR in [15]. Also, Posicast and P+Resonant controllers can be used to improve the transient response and eliminate the steady-state error in DVR. The Posicast controller is a kind of step function with two parts and is used to improve the damping of the transient oscillations initiated at the start instant from the voltage sag. The state feed forward and feedback methods [17], symmetrical components estimation [18], robust control [19], and wavelet transform [20] have also been proposed as different methods of controlling the DVR.

In all of the aforementioned methods, the source of disturbance is assumed to be on the feeder which is parallel to the DVR feeder. In this paper, a multifunctional control system is proposed in which the DVR protects the load voltage using Posicast and P+Resonant controllers when the source of disturbance is the parallel feeders. On the other hand, during a downstream fault, the equipment protects the PCC voltage, limits the fault current, and protects itself from large fault current. Although this latest condition has been described in [11] using the flux control method, the DVR proposed there acts like a virtual inductance with a constant value so that it does not receive any active power during limiting the fault current. But in the proposed method when the fault current passes through the DVR, it acts like a series variable impedance (unlike [11] where the equivalent impedance was a constant).

The basis of the proposed control strategy in this paper is that when the fault current does not pass through the DVR, an outer feedback loop of the load voltage with an inner feedback loop of the filter capacitor current will be used. Also, a feedforward loop will be used to improve the dynamic response of the load voltage. Moreover, to improve the transient response, but in case the fault current passes

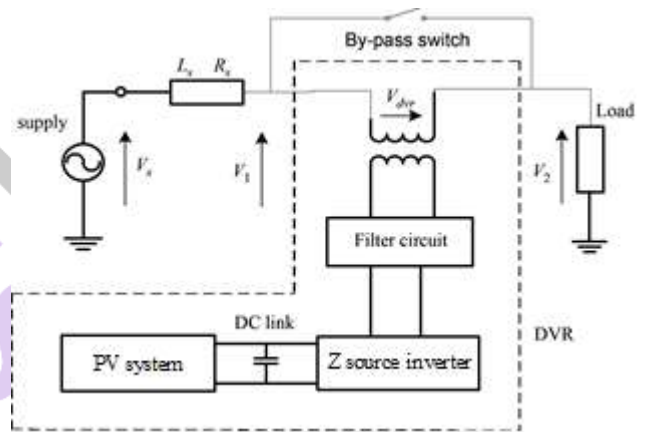


Fig. 1. Typical DVR-connected distribution system.

Through the DVR, using the flux control algorithm [11], the series voltage is injected in the opposite direction and, therefore, the DVR acts like a series variable impedance.

The remainder of this paper is organized as follows: The general operation of DVR and its state space description are provided in Section II. The closed-loop control using Posicast and P+Resonant controller has been presented in Section III. In Section I, the multifunctional DVR is introduced. The basis of the proposed control method is described in Section V. Finally, the simulation results are provided in Section VI which show that the control capability of the proposed DVR system is satisfactory.

PHOTOVOLTAIC SYSTEMS

A Photovoltaic (PV) system directly converts sunlight into electricity. The basic device of a PV system is the PV cell. Cells may be grouped to form panels or arrays. The voltage and current available at the terminals of a PV device may directly feed small loads such as lighting systems and DC motors. [7] A photovoltaic cell is basically a semiconductor diode whose p-n junction is exposed to light. Photovoltaic cells are made of several types of semiconductors using different manufacturing processes. The incidence of light on the cell generates charge carriers that originate an electric current if the cell is short circuited.

The equivalent circuit of PV cell is shown in figure 5. In the diagram the PV cell is represented by a current source in parallel with diode. R_s and R_p represent series and parallel resistance respectively.

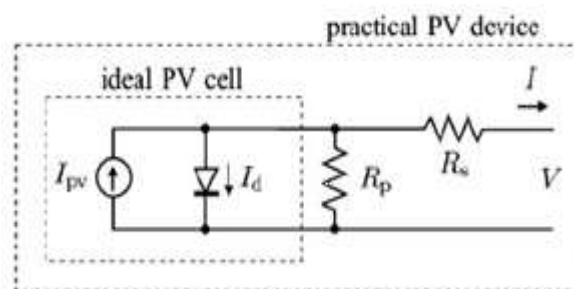


Figure.2. Equivalent Circuit of a PV Device

Z SOURCE INVERTER

The Z source inverter is a single stage converter that can either buck or boost the ac output voltage from add supply. This topology overcomes the shortcomings of the traditional voltage source and current source inverters, where the output ac voltage is either respectively less or more than the input dc voltage. This combined operation of the source inverter eliminates the need of a separate dc-dc converter, thus reducing the cost and increasing the efficiency of the circuit. Z source inverter also allows two switches of the same leg to be gated in the circuit, thus eliminating the shootthrough fault that occurs in traditional converters. This feature of the inverter provides the elimination of dead time in the circuit, thus increasing the reliability and reducing the output distortion of the inverter. Saying that does not free the Z source inverter from few of its operating problems - the voltage across the capacitors in the traditional Z source inverter is equal to the input voltage which increases the volume and cost of the capacitors used; and also the start-up current and voltage in the circuit is very much higher which may destroy the devices at one time or the other. So to overcome the above said problems, a new topology of the Z source inverter is used, that can be used to drive an induction motor and to control its operating speed.

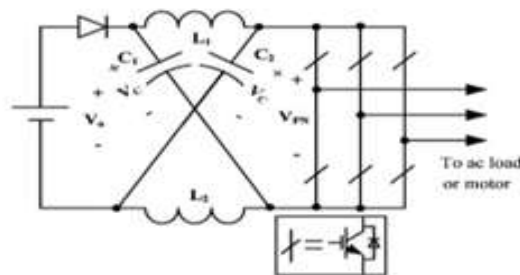


Fig.3. Z Source Inverter

A unique impedance network is used in the Z source inverter that consists of two identical inductors L_1 and L_2 along with two identical capacitors C_1 and C_2 that couples the power supply circuit to the inverter circuit. The shoot through period i.e., the time period when two switches of the same leg are gated allows the voltage to be boosted to the required value when the input dc voltage is not up to the required level. Else otherwise, the shoot through state is not used thus enabling the ZSI to operate as both a buck-boost inverter unlike the traditional voltage source and the current source inverters.

Z-source inverter can boost dc input voltage with no requirement of dc-dc boost converter or step up transformer, hence overcoming output voltage limitation of traditional voltage source inverter as well as lower its cost. A comparison among conventional PWM inverter, dc-dc boosted PWM inverter, and Z-source inverter shows that Z-source inverter needs lowest semiconductors and control circuit cost, which are the main costs of a power electronics system. This results in increasing attention on Z-source inverter, especially for the application where the input DC source has a wide voltage variation range, such as the photovoltaic (PV) grid-tied generation and fuel cell motor drive system. Moreover, for Z-source inverter we have not to worry about EMI influence since shoot through are welcome and even exploited. This in turn enhances the inverter reliability.

There are various methods can be used to control Z-source inverter. These can be classified into two categories according to the different shoot-through (ST) states insertion methods. The first category has the principle that ST states are generated by properly level shifting the modulation signals of voltage source inverter. ST states then will be inserted at every states transition, six ST state insertions in one switching cycle.

II. DVR COMPONENTS AND ITS BASIC

OPERATIONAL PRINCIPLE

A. DVR Components

A typical DVR-connected distribution system is shown in Fig. 1, where the DVR consists of essentially a series-connected injection transformer, a voltage-source inverter, an inverter output filter, and an energy storage device that is connected to the dc link. Before injecting the inverter output to the system, it must be filtered so that harmonics due to switching function in the inverter are eliminated. It should be noted that when using the DVR in real situations, the injection transformer will be connected in parallel with a bypass switch (Fig. 1). When there is no disturbances in voltage, the injection transformer (hence, the DVR) will be short circuited by this switch to minimize losses and maximize cost effectiveness. Also, this switch can be in the form of two parallel thyristors, as they have high on and off speed [21]. A financial assessment of voltage sag events and use of flexible ac transmission systems (FACTS) devices, such as DVR, to mitigate them is provided in [22]. It is obvious that the flexibility of the

DVR output depends on the switching accuracy of the pulsewidth modulation (PWM) scheme and the control method. The PWM generates sinusoidal signals by comparing a sinusoidal wave with a sawtooth wave and sending appropriate signals to the inverter switches. A further detailed description about this scheme can be found in [23].

B. Basic Operational Principle of DVR

The DVR system shown in Fig. 1, controls the load voltage by injecting an appropriate voltage phasor (V_{dvr}) in series with

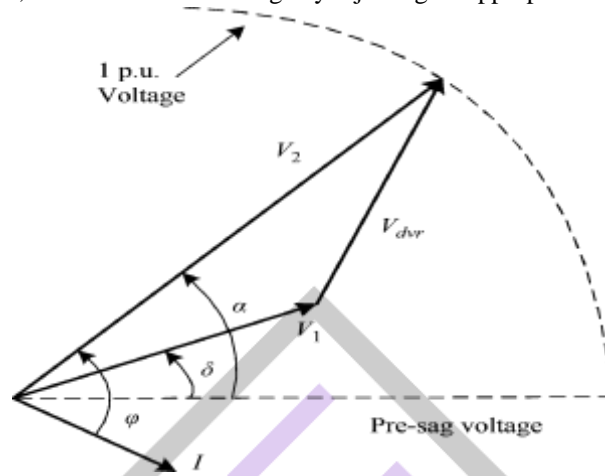


Fig. 4. Phasor diagram of the electrical conditions during voltage sag.

System using the injection series transformer. In most of the sag compensation techniques, it is necessary that during compensation, the DVR injects some active power to the system. Therefore, the capacity of the storage unit can be a limiting factor in compensation, especially during long-term voltage sags. PV system

The phasor diagram in Fig. 4, shows the electrical conditions during voltage sag, where, for clarity, only one phase is shown. Voltages, and are the source-side voltage, the load side voltage, and the DVR injected voltage, respectively. Also, the operators I , α , δ , and φ are the load current, the load power factor angle, the source phase voltage angle, and the voltage phase advance angle, respectively [24]. It should be noted that in addition to the in-phase injection technique, another technique, namely “the phase advance voltage compensation technique” is also used [24]. One of the advantages of this method over the in-phase method is that less active power should be transferred from the storage unit to the distribution system. This results in compensation for deeper sags or sags with longer durations.

Due to the existence of semiconductor switches in the DVR inverter, this piece of equipment is nonlinear. However, the state equations can be linearized using linearization techniques. The dynamic characteristic of the DVR is influenced by the filter and the load. Although the modelling of the filter (that usually is a simple LC circuit) is easy to do, the load modelling is not as simple because the load can vary from a linear time-invariant one to a nonlinear time-variant one. In this paper, the simulations are performed with two types of loads: 1) a constant power load and 2) a motor load.

As Fig. 5 shows, the load voltage is regulated by the DVR through injecting V_{dvr} . For simplicity, the bypass switch shown in Fig. 1 is not presented in this figure. Here, it is assumed that the load has a resistance R_L and an inductance. DVR harmonic filter has an inductance of L_f , a resistance of R_f , and a capacitance of C_f . Also, the DVR injection transformer has a combined winding resistance of R_t , a leakage inductance of L_t , and turns ratio of 1:n

The Posicast controller is used in order to improve the transient response. Fig. 4 shows a typical control block diagram of the DVR. Note that because in real situations, we are dealing with multiple feeders connected to a common bus, namely “the Point of Common Coupling (PCC),” from now on, and will be replaced with V_{PCC} and V_L , respectively, to make a generalized sense. As shown in the figure, in the open-loop control, the voltage on the source side of the DVR is compared with a load-side reference voltage so that the necessary injection voltage V_{inv}^* is derived. A simple method to continue is to feed the error signal into the PWM inverter of the DVR. But the problem with this is that the transient oscillations initiated at the start instant from the voltage sag could not be damped sufficiently. Where are the step response overshoot and the period of damped response signal, respectively? It should be noted that the Posicast controller has limited high-frequency gain; hence, low sensitivity to noise.

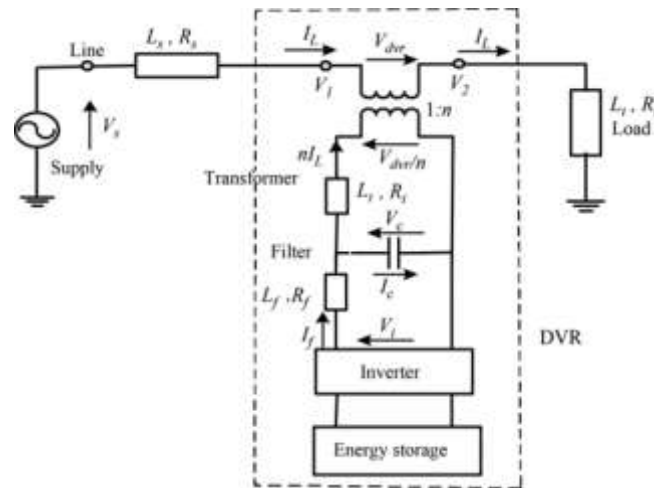


Fig. 5. Distribution system with the DVR.

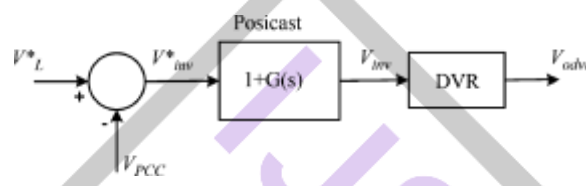


Fig. 6. Open-loop control using the Posicast controller.

To find the appropriate values of δ and T_d , first the DVR model will be derived according to Fig.3, as follows

$$1 + G(s) = 1 + \frac{\delta}{1 + \delta} (e^{-s \frac{T_d}{2}} - 1) \tag{1}$$

$$V_i = V_c + I_f R_f + L_f \frac{dI_f}{dt}$$

$$I_f = I_c + nI_t$$

$$I_c = C_f \frac{dV_c}{dt}$$

$$V_{dvr} = n[V_c - n(R_t I_t + L_t \frac{dI_t}{dt})]$$

$$V_2 = V_1 + V_{dvr} \tag{2}$$

Then, according to (2) and the definitions of damping and the delay time in the control literature, and are derived as follows:

$$T_d = \frac{2\pi}{\omega_r} = \frac{\pi}{\sqrt{\frac{1}{L_f C_f} - \frac{R^2}{4L_f^2}}}$$

$$\delta = e^{\frac{\epsilon\pi}{\sqrt{1-\epsilon^2}}} = e^{-R_f \pi \sqrt{C_f} / \sqrt{4L_f - R_f^2 C_f}} \tag{3}$$

The Posicast controller works by pole elimination, and proper regulation of its parameters is necessary. For this reason, it is sensitive to inaccurate information of the system damping resonance frequency. To decrease this sensitivity, as is shown in Fig. 5, the open-loop controller can be converted to a closedloop controller by adding a multiloop feedback path parallel to the existing feedforward path. Inclusion of a feedforward and a feedback path is commonly referred to as two-degrees-of-freedom (2-DOF) control in the literature. As the name implies, 2-DOF control provides a DOF for ensuring fast dynamic tracking through the

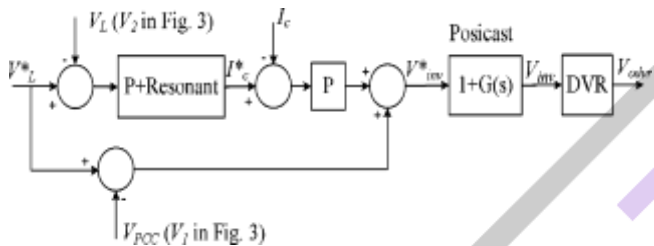
feedforward path and a second degree of freedom for the independent tuning of the system disturbance compensation through the feedback path [12]. The feedback path consists of an outer voltage loop and a fast inner current loop. To eliminate the steady-state voltage tracking error, $V_L^* - V_L$ computationally less intensive P+Resonant compensator is added to the outer voltage loop. The ideal P+Resonant compensator can be mathematically expressed as

$$G_R(s) = k_p + \frac{2k_I s}{S^2 + \omega_0^2} \tag{4}$$

k_P and k_I are gain constants and $\omega_0 = 2\pi \times 50$ rad/sec

the resonant controller compensates by introducing an infinite gain at the resonant frequency of 50 Hz (Fig. 6) to force the steady-state voltage error to zero. The ideal resonant controller, however, acts like a network with an infinite quality factor, which is not realizable in practice. A more practical (nonideal) compensator is therefore used here, and is expressed as

Plotting the frequency response of (5), as in Fig. 6, it is noted that the resonant peak now has a finite



gain of 40dB which is satisfactorily high for eliminating the voltage tracking error [12].

The large fault current will cause the PCC voltage to drop and the loads on the other feeders connected to this bus will be affected. Furthermore, if not controlled properly, the DVR might also contribute to this PCC voltage sag in the process of

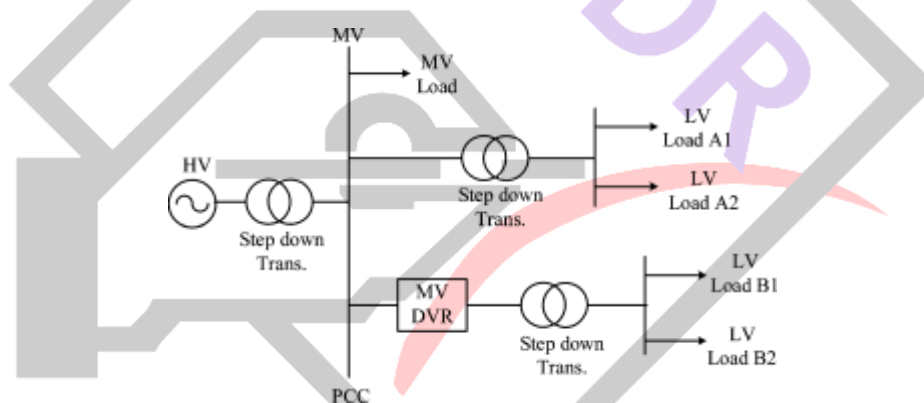


Fig. 7. DVR connected in a medium-voltage level power system.

Compensating the missing voltage, hence further worsening the fault situation [11].

To limit the fault current, a flux-charge model has been proposed and used to make DVR act like a pure virtual inductance which does not take any real power from the external system and, therefore, protects the dc-link capacitor and battery as shown in Fig. 1 [11]. But in this model, the value of the virtual inductance of DVR is a fixed one and the reference of the control loop is the flux of the injection transformer winding, and the PCC voltage is not mentioned in the control loop. In this paper, the PCC voltage is used as the main reference signal and the DVR acts like a variable impedance. For this reason, the absorption of real power is harmful for the battery and dc-link capacitor. To solve this problem, an impedance including a resistance and an inductance will be connected in parallel with the dc-link capacitor. This capacitor will be separated from the circuit, and the battery will be connected in series with a diode just when the downstream fault occurs so that the power does not enter the battery and the dc-link capacitor. It should be noted here that the inductance is used mainly to prevent large oscillations in the current. The active power mentioned is, therefore, absorbed by the impedance.

IV. PROPOSED METHOD FOR USING THE FLUX-CHARGE MODEL

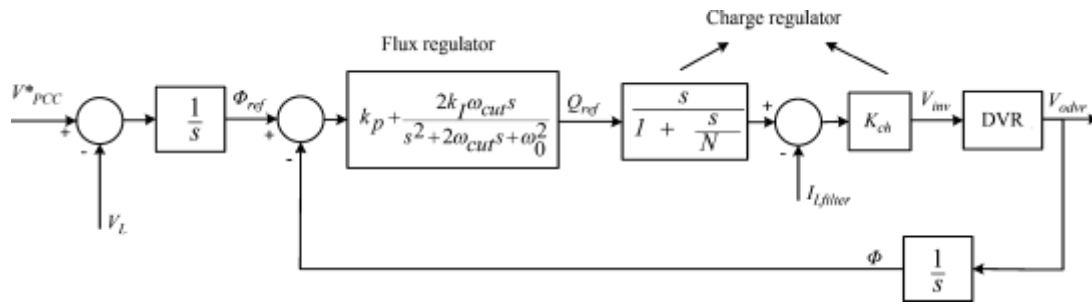


Figure 8 Multiloop control using the Posicast and P+Resonant controllers.

In this part, an algorithm is proposed for the DVR to restore the PCC voltage, limit the fault current, and, therefore, protect the DVR components. The flux-charge model here is used in a way so that the DVR acts as a virtual inductance with a variable value in series with the distribution feeder. To do this, the DVR must be controlled in a way to inject a proper voltage having the opposite polarity with respect to usual cases. It should be noted that overcurrent tripping is not possible in this case, unless additional communication between the DVR and the downstream side overcurrent circuit breaker (CB) is available. If it is necessary to operate the overcurrent CB at PCC, communication between the DVR and the PCC breaker might have to be made and this can be easily done by sending a signal to the breaker when the DVR is in the fault-current limiting mode as the DVR is just located after PCC [11]. The proposed DVR control method is illustrated in Fig. 8. It should also be noted that the reference flux (Φ_{ref}) is derived by integration of the subtraction of the PCC reference voltage (V_{PCC}^*) and the DVR load-side voltage. In this control strategy, the control variable used for the outer flux model is the inverter-filtered terminal flux defined as:

$$\Phi = \int V_{odvr} dt \tag{6}$$

Where V_{odvr} is the filter capacitor voltage of the DVR (at the DVR power converter side of the injection transformer). The flux error is then fed to the flux regulator, which is a P+Resonant controller, with a transfer function given in (6). On the other hand, it can be shown that a single flux-model would not damp out the resonant peak of the LC filter connected to the output of the inverter.

To stabilize the system, an inner charge model is therefore considered. In this loop, the filter inductor charge, which is derived by integration of its current, tracks the reference charge output Q_{ref} of the flux regulator. The calculated charge error is then fed to the charge regulator with the transfer function

$$G_{charge}(s) = k_{Ch} \frac{s}{1 + \frac{s}{N}} \tag{7}$$

Which is actually a practical form of the derivative controller. In this transfer function, the regulator gain is limited to N at high frequencies to prevent noise amplification.

The derivative term in $s/1 + s/N$ neutralizes the effects of voltage and current integrations at the inputs of the flux-charge model, resulting in the proposed algorithm having the same regulation performance as the multiloop voltage-current feedback control, with the only difference being the presence of an additional low-pass filter in the flux control loop in the form of . The bandwidth of this low-pass filter is tuned (through varying) with consideration for measurement noise attenuation, DVR LC-filter transient resonance attenuation, and system stability margins.

C. Starting the Induction Motor

A large induction motor is started on bus "03:MILL-1." The motor specifications are provided in Appendix C. The large motor starting current will cause the PCC voltage (bus "03:MILL-1" voltage) to drop. The simulation results in the case of using the DVR are shown in Fig. 11. In this simulation, the motor is started at $t = 405$ ms. as can be seen in Fig. 11, at this time, the PCC rms voltage drops to about 0.8 p.u. The motor speed reaches the nominal value in about 1 s.

During this period, the PCC bus is under voltage sag. From $t = 1.4$ s, as the speed approaches nominal, the voltage also approaches the normal condition. However, during all of these events, the DVR keeps the load bus voltage (bus "05: FDR F" voltage) at the normal condition. Also, as can be seen in the enlarged version of Fig. 11, the DVR has succeeded in restoring the load voltage in half a cycle from the instant of the motor starting.

D. Fault Current Limiting

The last simulation is run for an asymmetrical downstream fault, and the capability of the DVR to reduce the fault current and restore the PCC voltage is tested. For this purpose, a three-phase short circuit is applied on bus "05:FDR F". In Fig. 12, the fault current, without the DVR compensation, is shown.

For the simulation with DVR compensation, the three-phase fault is applied at $t = 205$ ms and then removed after 0.1 s. Also, a breaker will remove the faulted bus from the entire system at $t = 300$ ms. Fig. 13 shows the DVR operation during the fault. As can be seen, the rms load bus voltage reaches zero during the fault, and as the enlarged figure shows, in about half a cycle, the DVR has succeeded in restoring the PCC voltage wave shape to the normal condition. It should be noted that the amount and shape of the oscillations depend on the time of applying the fault. As Fig. 13 shows, at this time, the voltage value of phase B is nearly zero; this phase has the minimum has been reduced from 40 kA (see Fig. 12) to 5 kA with DVR compensation has been reduced from 40 kA (see Fig. 12) to 5 kA with DVR compensation.

Three-phase asynchronous motors can be considered among the most reliable electrical machines they carry out their function for many years with reduced maintenance and adapt themselves to different performances according to the requirements of both production as well as service applications. As already said, these motors find their application in the most different industrial sectors, such as food, chemical, metallurgical industries, paper factories or water treatment and extractive systems. The applications concern the equipment with machine components running at fixed or variable speed such as for example lifting systems as lifts or good hoists, transporting systems as conveyors, ventilation and air conditioning installations, without forgetting the commonest use with pumps and compressors. From the above considerations it is easily deduced how three-phase asynchronous motors can be considered the most widespread electric machine for industrial applications (the power consumption of electrical motors is about 75% of the total consumption in the industrial field).

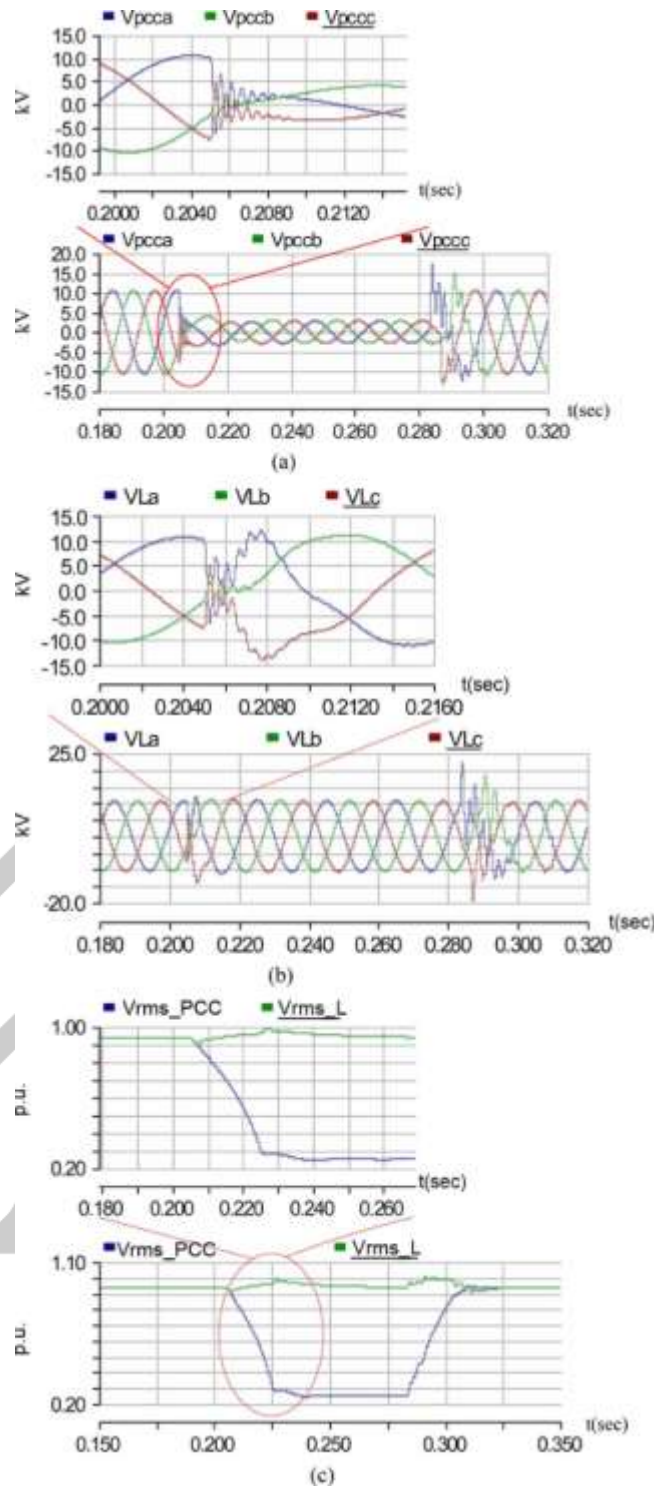


Fig. 10. Three-phase fault compensation by DVR. (a) Three-phase PCC voltages. (b) Three-phase load voltages. (c) RMS voltages of PCC and load.

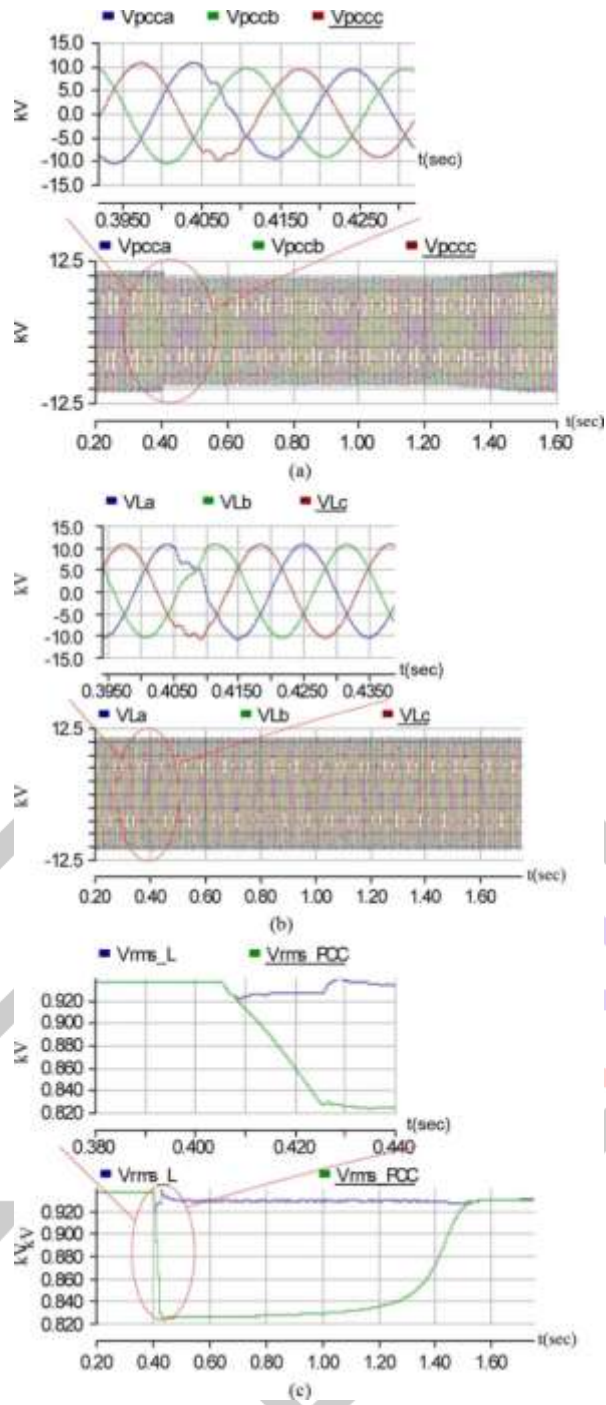


Fig. 11. Starting of an induction motor and the DVR compensation. (a) Three-phase PCC voltages. (b) Three-phase load voltages. (c) RMS voltages of PCC and load.

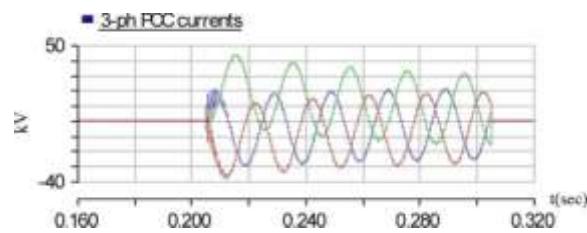


Fig. 12. Current waveshape due to the three-phase short-circuit fault without DVR compensation.

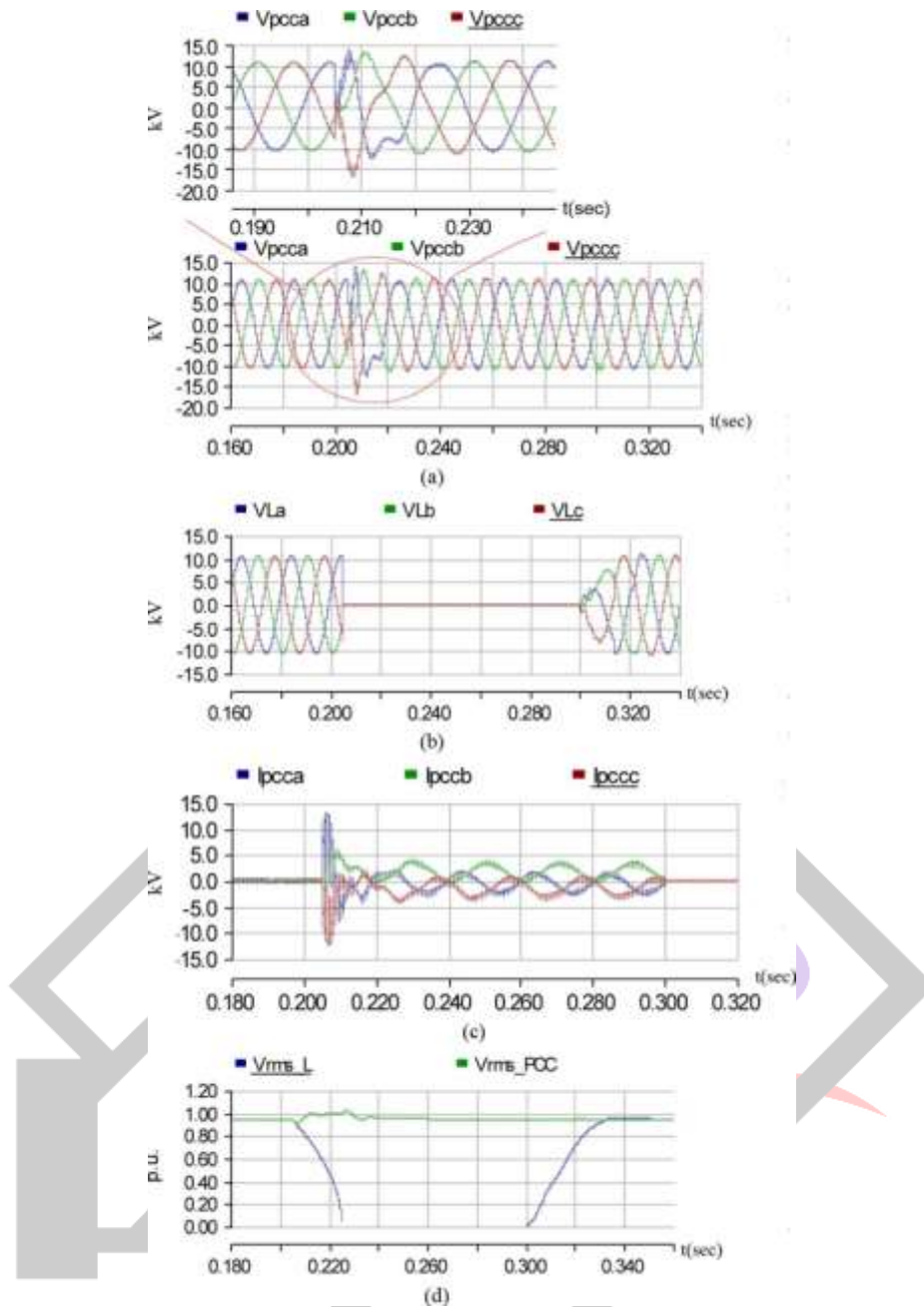


Fig. 13. Fault current limiting by DVR. (a) Three-phase PCC voltages. (b) Three-phase load voltages. (c) Three-phase currents. (d) RMS voltages of the PCC and load.

VI. CONCLUSION

In this paper, a multifunctional DVR is proposed, and a closed-loop control system is used for its control to improve the damping of the DVR response. Also, for further improving the transient response and eliminating the steady-state error, the Posicast and P+Resonant controllers are used. As the second function of this DVR, using the flux-charge model, the equipment is controlled so that it limits the downstream fault currents and protects the PCC voltage during these faults by acting as a variable impedance. The problem of absorbed active power is solved by entering an impedance just at the start of this kind of fault in parallel with the dc-link capacitor and the battery being connected in series with a diode so that the power does not enter it. The simulation results verify the effectiveness and capability of the proposed DVR in compensating for the voltage sags caused by short circuits and the large induction motor starting and limiting the downstream fault currents and protecting the PCC voltage.

APPENDIX

DVR

PARAMETERS:

$$(L_f] = 1 \text{ mH}$$

$$(C_f] = 700 \mu$$

Filter inductance
 Filter capacitanceF
 Inverter modulation ratio=21 mF
 Kind of DVR inverter: 12 Pulse
 DC-link capacitance: 26 mF
 Entered resistance for current limiting: 3 ohms
 Entered inductance for current limiting: 2 mH
 Supply battery: 12 kV.

Control System Parameters:

$$\delta = 1 \quad \begin{array}{l} T_d = 41.56 \mu \\ K_p = 1 \\ K_I = 100 \\ \omega_0 = 314 \quad \text{rad/s.} \\ \omega_{cut} = 1.0 \end{array}$$

Induction Motor Parameters: Rated power: 2.4 MVA
 Rated voltage: 13.8 kV
 Moment of inertia: 3.7267 sec
 Number of rotor squirrel cages: 1 Base frequency: 50 Hz
 Stator resistance: 0.0034 p.u. Rotor resistance: 0.298 p.u.
 Stator inductance: 0.0102 p.u. Rotor inductance: 0.05 p.u.
 Magnetizing inductance: 0.9 p.u.

REFERENCES

- [1] J. A. Martinez and J. Martin-Arnedo, "Voltage sag studies in distribution networks- part II: Voltage sag assessment," *IEEE Trans. Power Del.*, vol. 21, no. 3, pp. 1679–1688, Jul. 2006.
- [2] J. A. Martinez and J. M. Arnedo, "Voltage sag studies in distribution networks- part I: System modelling," *IEEE Trans. Power Del.*, vol. 21, no. 3, pp. 338–345, Jul. 2006.
- [3] P. Hcine and M. Khronon, "Voltage sag distribution caused by power system faults," *IEEE Trans. Power Syst.*, vol. 18, no. 4, pp. 1367–1373, Nov. 2003.
- [4] S. S. Choi, B. H. Li, and D. M. Vilathgamuwa, "Dynamic voltage restoration with minimum energy injection," *IEEE Trans. Power Syst.*, vol. 15, no. 1, pp. 51–57, Feb. 2000.
- [5] C. Fitzer, M. Barnes, and P. Green, "Voltage sag detection technique for a dynamic voltage restore," *IEEE Trans. Ind. Appl.*, vol. 2, no. 1, pp. 203–212, Jan./Feb. 2004.
- [6] C. Benachaiba and B. Ferdi, "Voltage quality improvement using DVR," *Electt. Power Qual. Utilisation, Journal*, vol. XIV, no. 1, 2008.
- [7] D. M. Vilathgamuwa, H. M. Wijekoon, and S. S. Choi, "A novel technique to compensate voltage sags in multilines distribution system-the interline dynamic voltage restorer," *IEEE Trans. Ind. Electron.*, vol. 53, no. 5, pp. 1603–1611, Oct. 2006.
- [8] J. G. Nielsen, M. Newman, H. Nielsen, and F. Blaabjerg, "Control and testing of a dynamic voltage restorer (DVR) at medium voltage level," *IEEE Trans. Power Electron.*, vol. 19, no. 3, pp. 806–813, May 2004.
- [9] M. J. Newman, D. G. Holmes, J. G. Nielsen, and F. Blaabjerg, "A dynamic voltage restorer (DVR) with selective harmonic compensation at medium voltage level," *IEEE Trans. Ind. Appl.*, vol. 41, no. 6, pp. 1744–1753, Nov./Dec. 2005.
- [10] A. K. Jindal, A. Ghosh, and A. Joshi, "Critical load bus voltage control using DVR under system frequency variation," *Elect. Power Syst. Res.*, vol. 78, no. 2, pp. 255–263, Feb. 2008.
- [11] Y. W. Li, D. M. Vilathgamuwa, P. C. Loh, and F. Blaabjerg, "A dualfunctional medium voltage level DVR to limit downstream fault currents," *IEEE Trans. Power Electron.*, vol. 22, no. 4, pp. 1330–1340, Jul. 2007.
- [12] P. C. Loh, D. M. Vilathgamuwa, S. K. Tang, and H. L. Long, "Multilevel dynamic voltage restorer," *IEEE Power Electron. Lett.*, vol. 2, no. 4, pp. 125–130, Dec. 2004.
- [13] E. Babaei, M. Farhadi, and M. Sabahi, "Compensation of voltage disturbances in distribution systems using single-phase dynamic voltage restorer," *Elect. Power Syst. Res.*, Jul. 2010.
- [14] C. N.-M. Ho and H. S.-H. Chung, "Implementation and performance evaluation of a fast dynamic control scheme for capacitor-supported interline DVR," *IEEE Trans Power Electron.*, vol. 25, no. 8, pp. 1975–1988, Aug. 2010.
- [15] M. Vilathgamuwa, A. A. D. R. Perera, and S. S. Choi, "Performance improvement of the dynamic voltage restorer with closed-loop load voltage and current-mode control," *IEEE Trans. Power Electron.*, vol. 17, no. 5, pp. 824–834, Sep. 2002.
- [16] Y. W. Li, P. C. Loh, F. Blaabjerg, and D. M. Vilathgamuwa, "Investigation and improvement of transient response of DVR at medium voltage level," *IEEE Trans. Ind. Appl.*, vol. 43, no. 5, pp. 1309–1319, Sep./Oct. 2007.

- [17] H. Kim and S. K. Sul, "Compensation voltage control in dynamic voltage restorers by use of feedforward and state feedback scheme," *IEEE Trans. Power Electron.*, vol. 20, no. 5, pp. 1169–1177, Sep. 2005.
- [18] M. I. Marei, E. F. El-Saadany, and M. M. A. Salama, "A new approach to control DVR based on symmetrical components estimation," *IEEE Trans. Power Del.*, vol. 22, no. 4, pp. 2017–2024, Oct. 2007.
- [19] Y. W. Li, D. M. Vilathgamuwa, F. Blaabjerg, and P. C. Loh, "A robust control scheme for medium-voltage-level DVR implementation," *IEEE Trans. Ind. Electron.*, vol. 54, no. 4, pp. 2249–2261, Aug. 2007.
- [20] S. A. Saleh, C. R. Moloney, and M. A. Rahman, "Implementation of a dynamic voltage restorer system based on discrete wavelet transforms," *IEEE Trans. Power Del.*, vol. 23, no. 4, pp. 2360–2375, Oct. 2008.
- [21] H. Awad, J. Svensson, and M. Bollen, "Mitigation of unbalanced voltage dips using static series compensator," *IEEE Trans Power Electron.*, vol. 19, no. 3, pp. 837–846, May 2004.
- [22] J. V. Milanovic and Y. Zhang, "Global minimization of financial losses due to voltage sags with FACTS based devices," *IEEE Trans. Power Del.*, vol. 25, no. 1, pp. 298–306, Jan. 2010.
- [23] M. H. Rashid, *Power Electronics-Circuits, Devices and Applications*, 3rd ed. India: Prentice-Hall of India, Aug. 2006.
- [24] M. Vilathgamua, A. A. D. R. Perara, S. S. Choi, and K. J. Tseng, "Control of energy optimized dynamic voltage restorer," in *Proc. IEEE IECON Conf.*, San Jose, CA, 1999, vol. 2, pp. 873–878.
- [25] "Task force on harmonics modeling & simulation (co-author), test systemsforharmonics modelling andsimulation," *IEEE Trans Power Del.*, vol. 14, no. 2, pp. 579–585, Apr. 1999.



Vinaykumar Kwasborn in Relakunta, Telanganain1989 and he completed his B.Techin Electrical andElectronicsEngineeringfrom BITS, Narsampet in the year2011and the M.Techdegree from CVSR,Hyderabadin 2015.Presently,heis workingas anAssistant Professorin Bhoj Reddy EngineeringCollege for Women, Hyd.HisareasofinterestInclude PowerSystems,andPower Electronics.



Gundu Poornawasborn in Nizamabad, Telanganain1991 and she completed herB.Techin Electrical andElectronics Engineering from SSJEC, Vatinagula Pallyin the year2012and the M.Techdegree from BVRIT, Hyderabadin 2014.Presently, she isworkingas anAssistant Professorin Bhoj Reddy EngineeringCollege for Women, Hyd. Herareasofinterestinclude PowerSystems,and Power Electronics.